## **International Food Research Journal 32(3): 776 - 788 (June 2025)**

Journal homepage: http://www.ifrj.upm.edu.my



# Calcium-alginate microencapsulation of fruit juices: Investigation of factors affecting bead physical properties

<sup>1,2</sup>Pablo, A. G. P., <sup>1</sup>Klinkesorn, U. and <sup>1</sup>\*Tongchitpakdee, S.

<sup>1</sup>Department of Food Science and Technology, Faculty of Agro-Industry,

Kasetsart University, 10900 Bangkok, Thailand

<sup>2</sup>Department of Home Economics, College of Agriculture, Forestry and Environmental Sciences,

Western Philippines University, Aborlan, 5302 Palawan, Philippines

#### **Article history**

## Received: 2 January 2025 Received in revised form: 20 May 2025 Accepted: 22 May 2025

#### **Keywords**

gel strength,
bead size,
bead sphericity,
variable screening,
calcium alginate encapsulation,
Box-Hunter-and-Hunter
fractional factorial design

#### **Abstract**

Calcium-alginate microencapsulation (CAM) is regarded as a highly promising encapsulation method, which is cost-effective, biodegradable, heat-stable, and remarkably user-friendly. Nevertheless, the application of these advancements for fresh fruit juices remains an area with limited exploration due to the complexity of juices that affects the gelling behaviour of alginate. The present work investigated the effects of selected formulation and process variables on the physical properties of calcium-alginate beads produced from melon (Cucumis melo L.) and Indian gooseberry (Phyllanthus emblica) juices. A two-level fractional factorial design was used to assess the influence of fruit type, juice concentration, sodium alginate content, calcium chloride concentration, nozzle temperature, and gelling time on bead diameter, sphericity factor, and gel strength. The bead diameter ranged from  $492.42 \pm 31.58$  to  $661.05 \pm 35.16$  µm, with the largest beads obtained from Indian gooseberry juice under higher calcium levels. The sphericity factor ranged from 0.03 to 0.23, indicating variability in bead shape influenced by the type of fruit juice, gelling conditions, and formulation parameters. Gel strength, measured as absolute positive area, varied significantly among the treatments, with values ranging from  $1.35 \pm 0.82$  to  $6.83 \pm 0.51$  g·s. Stronger gels were observed in beads formulated with melon juice such as higher calcium chloride content and shorter gelling time. The results highlighted the combined effects of juice matrix and processing conditions in determining the structural integrity and performance of alginate-encapsulated juice beads, which may be applied in functional food and nutraceutical systems.

DOI

https://doi.org/10.47836/ifrj.32.3.12

© All Rights Reserved

#### Introduction

Encapsulation has been proven to enhance the stability of bioactive compounds, making them more suitable for use as food additives for purposes such as nutrient addition and off-flavour masking, as well as for longer storage stability (Saifullah *et al.*, 2019; Chaudhary *et al.*, 2021; Marcillo-Parra *et al.*, 2021). It involves the protection of bioactive compounds using various methods such as spray-drying, freezedrying, coacervation, and extrusion technologies. To date, there have been different encapsulation techniques done with bioactive compounds; methods are chosen based on the characteristics of the material

and how they are applied – whether they are added to a food product or used for nutraceuticals.

An encapsulation technique gaining popularity for its versatility and effectiveness is calcium-alginate microencapsulation (CAM). This technique relies on ionic cross-linking to create a gel matrix. CAM is primarily utilised for encapsulating bioactive extracts and microbial cells (Chean *et al.*, 2021). Various studies have highlighted CAM's capability to encapsulate a wide range of compounds without requiring thermal processing (Tomé and da Silva, 2022; Machado *et al.*, 2022). However, its application to different core materials needs to be specifically studied because of varying core material properties

that may impact encapsulation efficiency, as well as the chemical and structural stability of the product.

While previous studies utilising CAM have successfully encapsulated bioactive compounds in the form of aqueous plant extracts, few have explored the direct encapsulation of fresh fruit juices, which have more complex compositions including organic acids, sugars, and polyphenols that can interfere with gel formation. This represents a critical gap in the literature, as fruit juices are commonly consumed, and hold potential as carriers of functional ingredients.

The mechanism of calcium-alginate gel formations involves calcium ions' strong affinity to alginate, creating a long-lasting chemical bond between two carboxyl groups on the polymer chains, resulting in forming "egg-box" conformations which leads to an insoluble network (Paoletti and Donati, 2022; Forysenkova *et al.*, 2023). The encapsulation technique mostly used is the extrusion method which consists of dropping an aqueous alginate solution into a gelling bath (Chan *et al.*, 2009). In this process, the encapsulation protocol should be specifically designed, taking into consideration the type of active ingredient that will be encapsulated and its future application.

Some studies have explored the investigation of the effects of different factors on specific plant extracts. The factors that are most cited to affect the quality of CAM are the concentration of core materials (Najafi-Soulari *et al.*, 2016; Essifi *et al.*, 2021; Demircan and Oral, 2023), the technique for encapsulating sodium alginate and CaCl<sub>2</sub> concentration (Roopa and Bhattacharya, 2008; Celli *et al.*, 2016; Liu *et al.*, 2021; Sharifi *et al.*, 2021), pH of solutions (Guo and Kaletunç, 2016; Chuang *et al.*, 2017), gelation time (Gholamian *et al.*, 2021), and droplet size (Aizpurua-Olaizola *et al.*, 2016).

Therefore, in the context presented earlier, the objective of the present work was to investigate the factors affecting the physical properties of microbeads made with calcium alginate crosslinking. Through this, the significant factors were investigated for further optimisation for the development of encapsulated fruit juices through CAM.

### Materials and methods

Raw materials and chemicals

Two types of fruit juice were used in this experiment: Indian gooseberry (Emblica officinalis)

and melon (*Cucumis melo* var. *cantalupensis*), representing low and high pH fruit juice, respectively.

Indian gooseberries were harvested from Kanchanaburi, Thailand. Fruits were kept at -18°C during storage, and thawed overnight at  $4 \pm 2$ °C before use. The juice was extracted using a hydraulic presser (Sakaya HP-10, Sakaya Machinery Co., Ltd., Thailand). Melons were purchased from a local supermarket in Bangkok, Thailand. Melon juice was extracted using an electric juicer. Both juices were pasteurised at 80°C for 15 s using a water bath. The pasteurised juice samples were stored at  $4 \pm 2$ °C. The pH of fresh melon juice was  $6.04 \pm 0.12$ , while Indian gooseberry had a pH of  $2.61 \pm 0.01$ . The total soluble solids (TSS) were  $6.03 \pm 0.06$ °Brix for melon, and  $10.27 \pm 0.06$ °Brix for Indian gooseberry.

Food-grade sodium alginate and CaCl<sub>2</sub> were purchased from Chemipan Corporation Co., Ltd., Thailand. Sodium hydroxide pellet was purchased from KemAus Pty. Ltd. (New South Wales, Australia).

# Characterisation of alginate-juice solutions

The fruit juices were diluted with deionised distilled water, and used as a medium to dissolve the alginate powder. The viscosity, pH, and total soluble solids (TSS) of juice-alginate mixtures were measured, alongside observations of precipitation and flowability. Precipitation was evaluated 1 h after solution preparation by visual inspection for the presence of precipitates. Flowability was assessed by observing the continuous flow of the juice-alginate mixtures through the nozzle of the encapsulator (BUCHI B-390 Labortechnik AG, Flawil, Switzerland). which was used for microencapsulation. Good flowability was indicated smooth and continuous flow of the solution, while poor flowability was indicated by interruptions or blockages, likely caused by factors such as precipitation or clogging.

The viscosity of solutions was determined following the method of İbanoğlu (2002) using a Brookfield Viscometer (RV DV-III Brookfield Engineering Laboratories, Middleboro, MA USA) with a UL adapter and a spindle number 00. The viscosity of the solutions was measured at room temperature with 10 rpm using 30 s of shearing. Meanwhile, the pH was measured using a benchtop pH Meter (Oakton® pH 700, Singapore), and total soluble solids (TSS) were measured using a digital refractometer (ATAGO, Japan).

Variable screening using Box, Hunter and Hunter design

In this investigation, several input variables that may affect the formation of calcium-alginate microbeads were initially identified. The fractional factorial design 2\*\*(K-p) (Box and Hunter, 1961) was generated in a Box, Hunter and Hunter order, with six variables and eight runs using the Statistica (Version 14.0.0.15) Software (TIBCO Software Inc., Santa Clara, USA). The six independent variables selected were the type of fruit juice (X1), juice concentration (X2), alginate concentration (X3), CaCl<sub>2</sub> concentration (X4), nozzle temperature (X5), and gelling time (X6). The selection of these variables

was based on preliminary studies and a review of previous literatures. Table 1 shows the experimental factors, the minimum and maximum levels used, and the unique combination of factorial levels used in every run of the study based on Box, Hunter and Hunter order.

The Box, Hunter and Hunter matrix is one of the fractional factorial designs used in product developmental studies (Muñiz-Márquez *et al.*, 2016; Buenrostro-Figueroa *et al.*, 2017), in which the effect of all factors is screened first before proceeding with optimisation. This initial screening stage is crucial as it provides valuable insights into which factors warrant further investigation during optimisation.

Table 1. Minimum and maximum levels plotted in Box, Hunter and Hunter matrix experimental design.

Experimental design								
Factor code	Fa	ctor	Low level (-1)		U	level 1)		
X1	Frui	t type	Me	elon	Indian go	oseberry		
X2	Fruit juic	ee (%, v/v)	1	0	2	5		
X3	Sodium algi	nate (%, w/v)	0	.5	1	l		
X4	Nozzle tem	perature (°C)	2	2.5	4	0		
X5	CaCl <sub>2</sub> (	(%, w/v)		1	4	5		
X6	Gelling t	time (min)	2	20	12	20		
Run	X1	<b>X2</b>	<b>X3</b>	<b>X4</b>	X5	<b>X6</b>		
1	-1	-1	-1	+1	+1	+1		
2	-1	-1	+1	+1	-1	-1		
3	-1	+1	-1	-1	+1	-1		
4	-1	+1	+1	-1	-1	+1		
5	+1	-1	-1	-1	-1	-1		
6	+1	-1	+1	-1	+1	-1		
7	+1	+1	-1	+1	-1	-1		
8	+1	+1	+1 +1		+1	+1		

Preparation of calcium-alginate microbeads

The cross-linking solution was prepared by dissolving CaCl<sub>2</sub> in deionised distilled water, while the juice-alginate mixture was produced by diluting juice samples, and adding sodium alginate with constant stirring at 400 rpm for 1 h or until complete dissolution. The alginate-juice mixtures were then sonicated (Crest ultrasonics, Model RK 52, Berlin, Germany) for 15 min to remove air bubbles. Calcium alginate microbeads were prepared using a vibrating encapsulator following a modified protocol described by de Moura *et al.* (2018) and the equipment manual.

The encapsulator was set up using a 300  $\mu$ m nozzle system, a frequency of 700 Hz, an electrode at 1,500 V, a pressure of 500 - 600 mbar, and an amplitude of 2.0. Approximately, 100 mL of the

juice-alginate mixture was gently dispensed into 100 mL of the  $CaCl_2$  cross-linking solution to form alginate beads with a stirring rate of 100 rpm. The beads were allowed to undergo internal gelation during a defined gelling time. Subsequently, the beads were separated from the  $CaCl_2$  cross-linking solution by filtration through a fine nylon mesh (100  $\mu$ m), and were rinsed with 100 mL of deionised distilled water to stop the gelling process. Beads were contained in amber bottles, and stored at  $4\pm2^{\circ}C$  prior to analysis.

Determination of physical properties of CAM Bead size

The size (diameter) of CAMs was determined using a light microscope (Axio Imager A1, Carl

Zeiss, Oberkochen, Germany). Samples were placed on a microscope slide, and the images were recorded using the Image Pro software. The measurement tool of the software was also used to measure the maximum and perpendicular diameter of the beads. Maximum diameter was reported as the bead size (Y1).

## Sphericity

The sphericity of CAMs was assessed based on the computation of the sphericity factor (SF) to quantify the roundness of the beads (Y2). It was computed following the method of Azad *et al.* (2020), using Eq. 1:

$$SF = ((Dmax - Dper)/(Dmax + Dper))$$
 (Eq. 1)

where, Dmax = maximum diameter passing through a bead centroid ( $\mu$ m), and Dper = diameter perpendicular to the Dmax passing through the bead centroid. A zero SF represents a perfect sphere, while a higher absolute SF indicates a higher shape distortion. Thirty beads were randomly selected from each experimental run, and the experiment was replicated twice.

## Gel strength

A texture analysis following the method described by Bhujbal *et al.* (2014) with some modifications was used in this study. A Texture Analyzer plus C (Stable Micro Systems, Godalming, UK) with a load cell of 500 g was used to measure the mechanical stability of beads by compressing each bead onto a flat platform. Thirty beads were measured from each experimental run, and the experiment was replicated twice.

The measuring geometry consisted of a cylindrical aluminium probe (6 mm diameter) which was driven to compress the sample with a pre-test speed of 0.5 mm/s, a test speed of 0.01 mm/s, and a post-test speed of 2 mm/s. The trigger force was set to 2 g. The uniaxial compression test was initiated as the probe pressed the bead's surface. The force exerted by the probe (g) to compress the bead was recorded as a function of time (s) and computed as the absolute positive area (g.s); this represented the microbead gel strength, Y3. The probe was set to return to the original position immediately after compression. Texture Exponent Connect software version 6.0 was used for recording and analysing the data.

Statistical analysis

A multiple regression analysis was performed using the DOE procedure of Statistica (Version 14.0.0.15) Software (TIBCO Software Inc., Santa Clara, USA) to fit the following linear equation, Eq. 2:

$$Y = \beta_o + \Sigma \beta_i X_i \tag{Eq. 2}$$

where, Y = response,  $\beta o = \text{independent variable}$ ,  $\beta_i = \text{linear coefficient}$ , and  $X_i = \text{level of independent}$  variable. To understand the effects of each factor in different parameters, mean plots were generated. Pareto charts were also generated to highlight which factors have the most substantial impact. All other data were subjected to analysis of variance (p value < 0.05), and the means were separated using Tukey's Honestly Significant Difference (HSD) test ( $\alpha = 0.05$ ).

#### Results and discussion

Characterisation of alginate-juice solutions

Varying concentrations of diluted juice (10, 25, 50, and 75%) containing alginate at 1% (w/v) were prepared by diluting the original juice (100%) with deionised distilled water, and by adding sodium alginate at 1% (w/v) (Table 1). Upon varying the concentrations of juices while preparing the alginate solution (1%, w/v), notable shifts in viscosity were observed (p < 0.05). Melon juice viscosity at different dilutions was more consistent as compared to Indian gooseberry juice which had significant changes in viscosity as dilution changed. As expected, the dilution of juices led to a significant reduction in total soluble solids (TSS), and a slight change in pH. Notably, even with these significant changes in both pH and TSS resulting from juice dilution, the distinct variations between the two juices remained evident.

When Indian gooseberry juice at 50, 75, and 100% (v/v) concentrations were used, gelation and precipitation occurred in juice-alginate solutions, which is not favourable, especially when using a small-size nozzle system. These findings agreed with Celli et al. (2016), in which it was mentioned that there is a need to adjust the pH of the haskap berries aqueous extract from 2.9 to 4.5 before mixing with sodium alginate, which is essential to prevent the immediate gelation of the solution. Andriamanantoanina and Rinaudo (2010) highlighted the ability of alginate to form gels in acidic

conditions. Accordingly, for purified commercial alginate, a gel can be formed at solutions at pH < 3.05. Draget and Taylor (2011) further explained that alginate has the characteristic of forming acid gels at pH values below the pKa value of the uronic acid residues. One way to prevent this problem is to adjust the pH of the juice, so there will be no problem with alginate solution preparation and workability. As a result, the juice concentrations of 10 and 25% (v/v), for minimum and maximum levels, respectively, were used during variable screening.

## Variable screening

A fractional factorial design was employed following the Box, Hunter and Hunter matrix generated by the Statistica software to investigate the effects of six different factors on the formation of juice microbeads made through calcium-alginate ionic crosslinking. The six factors investigated were fruit type (X1), fruit juice concentration (X2), sodium alginate concentration (X3), nozzle temperature (X4), calcium chloride concentration (X5), and gelling time (X6). Responses that were investigated were bead size (Y1), bead sphericity (Y2), and bead gel strength (Y3), which are crucial factors for many applications, for they can indicate the microbead's stability (Partovinia and Vatankhah, 2019; Demircan and Oral, 2023). The size of the beads can affect various properties such as encapsulation efficiency, loading capacity, swelling, production yield, and release profile of the encapsulated compound (Bilal and Asgher, 2015; Berninger et al., 2016; Ta et al., 2022). A more spherical bead also means that the beads have a stronger gel structure which can hold the microbeads' shape. Absolute positive area, on the other hand, is a response that reflects the mechanical strength of the gels formed (Bhujbal et al., 2014), which is an essential parameter for microbead incorporation into products.

Table 2 shows the summary of responses for all the runs. Based on ANOVA, all factors exhibited significant effect (p < 0.05) on all responses, which means that all factors could contribute to the variability of bead characteristics. The results of both responses were analysed through linear regression to estimate the effects on F- and p-values of independent variables. When the coefficient is positive (+), it signifies that an increase in the levels of these factors will increase the response being studied. On the other hand, a negative (-) coefficient indicates that an

increase in these factors will lead to a decrease in the observed response.

The visual representation and ranking of each factor's contribution to the variations of responses are shown in Figure 1 using the Pareto charts generated by Statistica. Pareto charts are valuable tools for identifying the most influential factors impacting a response variable by visually representing their effect sizes. It provides a visual representation of the factors within a process, and ranks them in order of influence from the most significant to the least significant. However, it is important to note that fractional factorial designs cannot capture the interactions between factors, and may not provide an optimal solution. This design was utilised to understand the effect of each factor to the parameters studied.

Influence of type of fruit juices and different concentrations on CAM

The choice of the specific fruit types was grounded in the variations of pH levels across diverse fruit juices. For instance, Indian gooseberry was chosen as an example of a low-pH juice, while melon was representative of a juice with a neutral pH. This selection allowed for the inclusion of two distinct representatives from the spectrum of pH ranges of fruit juices for the screening experiment. Pure juices before adding alginate had a pH of  $6.04 \pm 0.12$  for melon, and  $2.61 \pm 0.01$  for Indian gooseberry, and TSS were  $6.03 \pm 0.06$  and  $10.27 \pm 0.06$ °Brix, respectively.

Based on ANOVA (Table 2), the type of fruit significantly influenced all the responses measured (p < 0.05). The findings revealed that the utilisation of distinct types of fruits could yield varying effects on the size and formation of microbeads. Specifically, employing a high pH fruit juice, exemplified by melon juice, resulted in the production of smaller and more spherical beads, characterised with higher gel strength. This indicated that beads created with melon juice exhibited a more stable shape and greater strength compared to those formed using acidic juice such as Indian gooseberry, as shown in Figure 2. It was observed that beads made with melon juice were more spherical compared to Indian gooseberry which were more irregular in shape. This observed correlation between juice type and concentration on bead characteristics agreed with the findings of Chuang et al. (2017), who demonstrated the influence of pH on bead morphology. Their study indicated that

**Table 2.** Actual values of experimental design and observed results of responses and analysis of variance. Values presented are mean ± SD (n = 60).

Run	Fruit type	Fruit juice (%, v/v)	Sodium alginate (%, w/v)	Nozzle temperature (°C)	CaCl <sub>2</sub> (%, w/v)	Gelling time (min)	Bead diameter (um)	Sphericity factor	Absolute positive area (g.s)
ı	X1	X2	X3	X4	X5	9X	Y1	Y2	Y3
	Melon	10	0.5	40	5	120	$498.66 \pm 34.22^{\mathrm{dB}}$	$0.06\pm0.04^{bcA}$	$1.93\pm0.54^{\mathrm{dB}}$
7	Melon	10		40	П	20	$571.27 \pm 50.49^{dB}$	$0.03 \pm 0.02^{bcA}$	$6.83\pm0.51^{\mathrm{eB}}$
$\epsilon$	Melon	25	0.5	25	5	20	$492.42 \pm 31.58^{dB}$	$0.06\pm0.05^{bcA}$	$2.19\pm0.30^{dB}$
4	Melon	25		25	П	120	$560.84 \pm 15.56^{\mathrm{dB}}$	$0.03\pm0.02^{\mathrm{aA}}$	$5.47\pm0.60^{\mathrm{cB}}$
5	Indian gooseberry	10	0.5	25		20	$516.11 \pm 40.40^{bcA}$	$0.06\pm0.05^{\mathrm{cB}}$	$1.35\pm0.82^{\mathrm{aA}}$
9	Indian gooseberry	10	_	25	5	20	$591.35 \pm 61.73^{bA}$	$0.05\pm0.0^{\rm bcB}$	$5.29\pm0.48^{bA}$
7	Indian gooseberry	25	0.5	40		120	$513.62\pm80.32^{\mathrm{cA}}$	$0.23 \pm 0.12^{\mathrm{cB}}$	$3.77\pm1.85^{bA}$
∞	Indian gooseberry	25		40	S	120	$661.05 \pm 35.16^{aA}$	$0.08\pm0.04^{bB}$	$4.20\pm0.56^{\mathrm{cA}}$

		Result of analysis of variance	sis of variance			
	(Y1) Bead di	Bead diameter (um)	(Y2) Spher	(Y2) Sphericity factor	(Y3) Absolut	(Y3) Absolute positive area
	Coefficient	Significance	Coefficient	Significance	Coefficient	Significance
Intercept, $eta_0$	552.258	* *	0.071	* * *	3.710	* * *
Fruit type, X1	42.928	* *	0.051	* *	-0.790	* *
Fruit juice (%, v/v), X2	9.444	*	0.057	* *	0.390	* * *
Sodium alginate (%, w/v), X3	87.737	* * *	-0.047	* * *	3.475	* * *
Nozzle temperature (°C), X4	17.780	* * *	0.057	* *	0.946	* * *
$CaCl_2$ (%, w/v), X5	17.223	* *	-0.021	* *	-0.613	* * *
Gelling time (min), X6	12.761	*	-0.030	* *	-1.350	* *

Data are mean  $\pm$  SD from analysis of each experimental run. Mean  $\pm$  SD values in similar column with different lowercase superscripts denote significant difference (p < 0.05) comparing all runs. Mean  $\pm$  SD values in similar column with different uppercase superscripts denote significant difference (p < 0.05) comparing two juices.

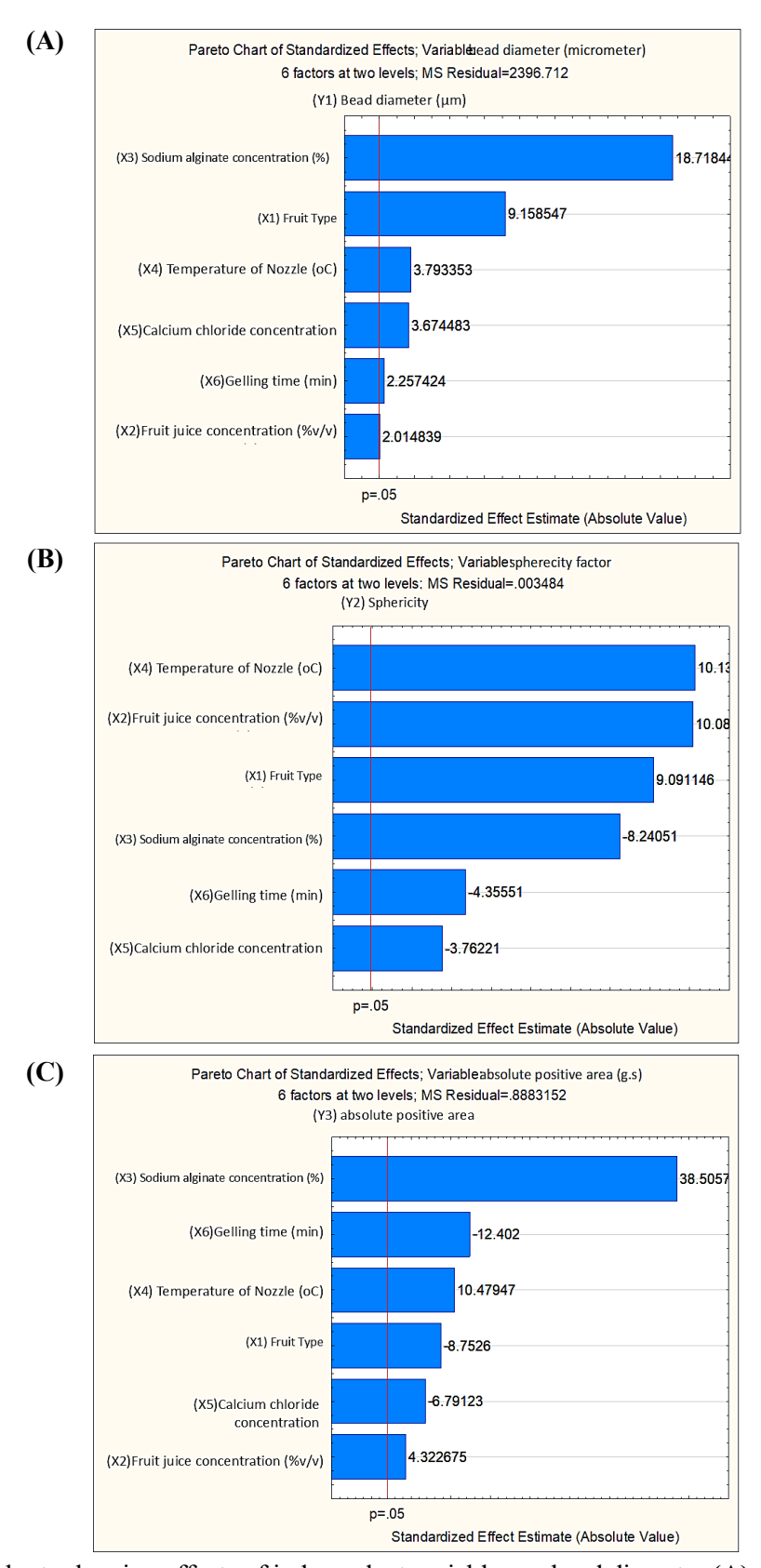


**Figure 1.** Pareto charts showing effects of independent variables on bead diameter **(A)**, sphericity **(B)**, and absolute positive area **(C)**.

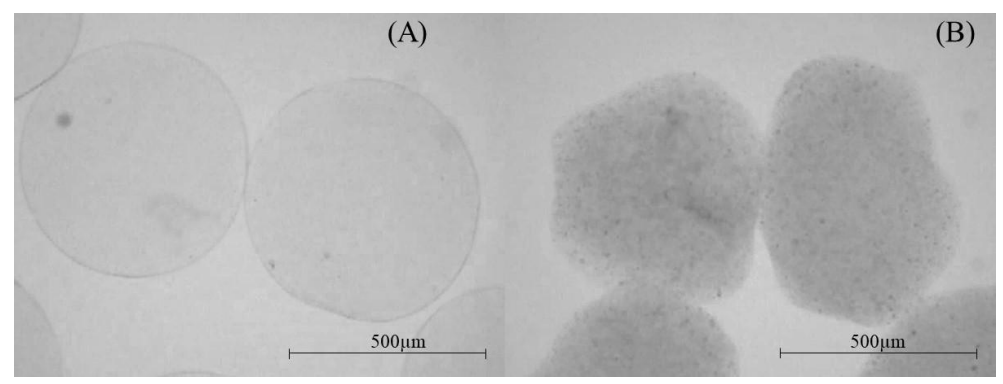


**Figure 2.** Calcium-alginate microbeads produced with different fruit juice (25%, w/v) with 1% (w/v) alginate (A), melon (B), and (C) Indian gooseberry at 40× magnification.

at pH 1, an alginate solution loaded with Coomassie brilliant blue G-250 produced oblate-shaped microbeads, whereas those prepared at pH 4, 7, and 10 exhibited a more spherical shape. The alginate particle shape is tailored by the balance between the polymer viscosity and the interfacial tension. In the present work, however, it was observed that the fruit juice type affected the viscosity of the alginate solution. Where melon was used, the viscosity of solutions was consistent. Variations were observed when Indian gooseberry juice was used, as mentioned previously.

These results also highlighted the importance of adjusting the pH level, especially when utilising CAM for highly acidic fruit juices. To achieve optimal bead morphology, particularly for acidic juices, it was thus recommended to increase the pH level, thus ensuring a more spherical shape with stronger gel strength.

The investigation into the influence of juice concentrations was also studied. The ANOVA revealed significant effects of all factors on the responses (p < 0.05). The findings demonstrated that lower concentrations of juice resulted in smaller spherical beads, and lower absolute positive area. However, making generalisations about distinctions between concentrations, especially when comparing the two juices, requires caution. To explore further the concentration effect on bead formation, responses were analysed using Tukey's Honestly Significant Difference (HSD) test. The results highlight the significant differences in microbeads produced from different fruit juices across all responses (Table 2). Specifically, runs 1 to 4 utilised melon juice, while runs 5 to 8 employed Indian gooseberry juice. Results revealed that beads made with melon juice exhibited minimal variance in bead size and sphericity compared to those made with Indian gooseberry

juice. A specific comparison between runs 6 and 8, which utilised Indian gooseberry juice with the same alginate concentration but different fruit juice concentrations, indicated that lower concentrations produced beads with smaller diameters, increased sphericity, and higher gel strength. This relationship suggested that the results were tied to the pH of the juice, as the dilution of Indian gooseberry juice substantially increased its рН (Table Consequently, this emphasised the significance of considering juice pH before preparing the alginate solution.

Influence of alginate and calcium chloride concentrations on CAM

Sodium alginate and CaCl<sub>2</sub> levels have been commonly examined as crucial factors in most microencapsulation studies (Song *et al.*, 2015; Valente *et al.*, 2019; Sharifi *et al.*, 2021). The concentration of CaCl<sub>2</sub> in the bath affects the gelation process and the shape of the beads (Bahraman and Alemzadeh, 2017). The concentration of alginate in the solution also plays a role in the formation of spherical beads. According to previous studies, higher concentrations of alginate can result in more spherical beads (Woo *et al.*, 2007; Zakeri *et al.*, 2019). However, preliminary investigation has shown that for a 300 µm nozzle to work with the specific alginate sample, a concentration of sodium alginate at not more than 1.1% (w/v) was recommended.

Based on ANOVA results, sodium alginate concentration significantly contributed to the variance of all responses (p < 0.05; Table 2). The results indicated that elevating sodium alginate levels led to the production of larger, more spherical beads with higher force required for compression. This implied that beads with higher sodium alginate levels exhibited enhanced stability in both form and texture.

Type of fruit juice	Juice concentration (%, v/v)	Viscosity (cP)	рН	TSS (°Brix)	Precipitation	Flowability of solution
	100	$427.00 \pm 87.64^{\rm NS}$	$6.56\pm0.01^{cd}$	$6.80\pm0.10^{\rm a}$	no	good
	75	$446.67 \pm 59.50$	$6.53\pm0.00^{\rm d}$	$5.03\pm0.06^b$	no	good
Malan	50	$449.67 \pm 88.71$	$6.61\pm0.04^{bc}$	$4.03\pm0.06^c$	no	good
Melon	25	$357.67 \pm 74.97$	$6.65\pm0.01^{b}$	$2.50\pm0.00^{d}$	no	good
	10	$420.67 \pm 110.61$	$6.70\pm0.01^{\rm a}$	$1.53\pm0.06^{\rm e}$	no	good
	0	$437.00 \pm 25.71$	$6.37\pm0.02^{\mathrm{e}}$	$1.50\pm0.10^{\rm e}$	no	good
	100	$7.25\pm0.37^{\rm c}$	$2.83\pm0.01^{\rm f}$	$10.30\pm0.00^{\mathrm{a}}$	yes	poor
Indian gooseberry	75	$36.93\pm2.58^{c}$	$2.93\pm0.01^{\text{e}}$	$7.83\pm0.06^{b}$	yes	poor
	50	$489.33 \pm 13.43^{\rm a}$	$3.18\pm0.01^{\text{d}}$	$5.53\pm0.06^{c}$	slight	poor
	25	$507.33 \pm 63.69^{a}$	$3.38 \pm 0.01^{\text{cd}}$	$3.47\pm0.06^{\rm d}$	no	good
-	10	$131.00 \pm 7.00^{b}$	$3.77\pm0.03^{\rm b}$	$2.37\pm0.06^{\text{e}}$	no	good
	$0^{1}$	$437.00 \pm 25.71^{a}$	$6.37 \pm 0.02^{e}$	$1.50 \pm 0.10^{\rm f}$	no	good

**Table 3.** Viscosity, pH, and TSS of alginate solutions at 1% (w/v) at different juice dilutions.

Data are mean  $\pm$  SD values from three experimental runs per sample. Mean  $\pm$  SD values in similar column with different lowercase superscripts denote significant difference (p value < 0.05) comparing within different juice concentrations. NS: not significant difference. <sup>1</sup>Aqueous alginate solution with 1% (w/v) sodium alginate.

This can be explained by the study of Bhujbal *et al.* (2014) where they discussed that the viscosity of alginate solution increased with higher concentrations of alginate solutions. They observed that alginate concentrations with lower viscosities produced easily ruptured beads.

Furthermore, the significance of CaCl<sub>2</sub> was evident across all responses (p < 0.05; Table 2). Findings demonstrated that an increase in CaCl<sub>2</sub> levels resulted in the formation of larger, more spherical beads with reduced gel strength. Despite the production of more spherical beads, those formed with high CaCl<sub>2</sub> exhibited lower gel strength. This phenomenon occurred due to the involvement of both alginate and calcium ions in the gelation mechanism, as explained by the egg-box model (Mazumder, 2013). Even with elevated levels, the formation of a cross-linked network still depends on the availability of carboxyl groups of alginate. Hence, results also highlighted the need for studying the combination of sodium alginate and CaCl<sub>2</sub> levels that will give the strongest bead system for encapsulation of different active materials.

# Influence of nozzle temperature on CAM

The influence of temperature on the gelation of calcium-alginate was also investigated in some studies (Jeong *et al.*, 2020; Haldar and Chakraborty, 2021). However, they emphasised the application of

heat on the crosslinking solution (calcium-containing solution). In the present work, the application of heat in the nozzle system was explored, and results showed that nozzle temperature had significant effect on all responses (p < 0.05; Table 2). Regression coefficients showed that smaller beads with a more spherical shape were produced with a lowertemperature nozzle. Higher gel strength can be produced with a higher temperature of the nozzle (Table 2). This can be explained by a previous study by Zhong et al. (2010), which confirmed that temperature affected alginate solution viscosity, wherein an increase in temperature decreased the solvation effect of polymer chains, which caused the alginate chain to move faster, hence affecting the behaviour of the alginate solution. Davarcı et al. (2017), on the other hand, explained in their study that to penetrate the CaCl<sub>2</sub> gelling bath, the alginate drop must have enough energy to break the surface of the gelling bath, which gives more emphasis on the importance of the viscosity of alginate solutions to form a more stable shape and bead structure. When the viscosity of the droplet is too low, the alginate droplet will spread out on the liquid surface, hence forming a less spherical bead.

## Influence of gelling time on CAM

Gelling time is defined as the incubation time of alginate gels in CaCl<sub>2</sub> solution, or in other words,

it refers to the duration and interaction between alginate and CaCl<sub>2</sub> ions (Ramdhan et al., 2019). Based on previous studies involving CAM, a wide range of gelling time was used in different studies ranging from 10 min to 3 h (Celli et al., 2016; Gholamian et al., 2021). Results of ANOVA showed that gelling time significantly affected all responses measured (Table 2). Based on the regression coefficients, increasing the gelling time increased bead size, and produced more spherical beads with lower gel strength, which implied that increasing the gelling time can decrease the mechanical stability of the beads. This agreed with Ramdhan et al. (2019) in the formation of cuboid calcium alginate gels. Their result highlighted that the strength of gels increased up to a certain level of time, and then decreased or became stable, hence emphasising the need to have another experiment that will optimise bead formation. Celli et al. (2016) in contrast, found that gelling time had no significant linear effect on bead size; hence, a minimum level of 10 min gelling time was chosen for their optimum condition encapsulating in anthocyanin extracts. Results recommended that the optimisation of gelling time on specific core materials must be studied extensively to obtain favourable results towards the parameters analysed.

## Model generation

A multiple regression analysis was performed based on the experimental data and estimated coefficients, which were used to develop linear equations that can be used to predict the responses. The equations in terms of actual levels are as follows:

$$Y1 = 552.26 + 42.93X_1 + 9.44X_2 + 87.74X_3 + 17.78X_4 + 17.22X_5 + 12.76X_6$$

$$Y2 = 0.07 + 0.05X_1 + 0.06X_2 - 0.05X_3 + 0.06X_4 -0.02X_5 - 0.03X_6$$

$$Y3 = 3.71 - 0.79X_1 + 0.39X_2 - 3.47X_3 + 0.95X_4$$
$$-0.61X_5 - 1.35X_6$$

The developed models described the relationships between the response variables (Y1, Y2, and Y3) and the six independent variables (X1 to X6). For Y1 (bead diameter), the model indicated that X3 had the most significant positive effect, followed by X1, while other variables contributed moderately. This suggested that Y1 was highly sensitive to

changes in X3 and X1. The model for Y2 revealed that X2 and X4 contributed positively but with small effects, while X3 had slight negative effect. The results indicated that Y2 was weakly influenced by the independent variables. For Y3, X3 had the most significant negative impact, followed by X6, while X4 contributed positively. This model highlighted the dominant negative role of X3 on Y3.

Moreover, it is important to note that PBD cannot capture the interactions between factors, and may not provide an optimal solution; hence, an optimisation study was suggested as the next part of the present work to fully explore the effects of interactions.

## Conclusion

In the present work, variables and their contribution to variability in calcium alginate microencapsulation of fruit juices were determined. In using highly acidic juices, the present work emphasised the need for juice dilution or pH adjustment for improved bead morphology and strength. Increasing the concentration of sodium alginate and calcium chloride, as well as gelling time, could also promote good bead structure and strength. Using a nozzle temperature of 25°C was also recommended. The size, sphericity, and mechanical stability of beads promoted storage and incorporation stability; however, the encapsulation efficiency of the core material should also be evaluated for optimum bead production. Further study should focus on process optimisation through response surface methodology (RSM) with encapsulation efficiency as a parameter and storage study of microbeads was recommended. Additionally, future research could explore the scalability of the encapsulation process, and explore the potential use of calcium-alginate microbeads in beverages or as carriers for bioactive compounds in functional food systems.

### Acknowledgement

The authors sincerely thank the German Academic Exchange Service (DAAD) and the Southeast Asian Regional Centre for Graduate Study and Research in Agriculture (SEARCA) for the scholarship and research support; the Western Philippines University for the study leave; and the Department of Food Science and Technology under

the Faculty of Agro-Industry, Kasetsart University, for providing invaluable research support in the completion of the present work.

#### References

- Aizpurua-Olaizola, O., Navarro, P., Vallejo, A., Olivares, M., Etxebarria, N., and Usobiaga, A. 2016. Microencapsulation and storage stability of polyphenols from *Vitis vinifera* grape wastes. Food Chemistry 190: 614-621.
- Andriamanantoanina, H. and Rinaudo, M. 2010. Characterization of the alginates from five Madagascan brown algae. Carbohydrate Polymers 82(3): 555-560.
- Azad, A. K., Al-Mahmood, S. M. A., Chatterjee, B., Wan Sulaiman, W. M. A., Elsayed, T. M. and Doolaanea, A. A. 2020. Encapsulation of black seed oil in alginate beads as a pH-sensitive carrier for intestine-targeted drug delivery: *In vitro*, *in vivo* and *ex vivo* study. Pharmaceutics 12(3): 219.
- Bahraman, F. and Alemzadeh, I. 2017. Optimization of L-asparaginase immobilization onto calcium alginate beads. Chemical Engineering Communications 204(2): 216-220.
- Berninger, T., Mitter, B. and Preininger, C. 2016. The smaller, the better? The size effect of alginate beads carrying plant growth-promoting bacteria for seed coating. Journal of Microencapsulation 33(2): 127-136.
- Bhujbal, S. V., Paredes-Juarez, G. A., Niclou, S. P. and de Vos, P. 2014. Factors influencing the mechanical stability of alginate beads applicable for immunoisolation of mammalian cells. Journal of the Mechanical Behavior of Biomedical Materials 37: 196-208.
- Bilal, M. and Asgher, M. 2015. Dye decolorization and detoxification potential of Ca-alginate beads immobilized manganese peroxidase. BMC Biotechnology 15: 1-14.
- Box, G. E. P. and Hunter, J. S. 1961. The 2<sup>k-p</sup> fractional factorial designs part II. Technometrics 3(4): 449-458.
- Buenrostro-Figueroa, J. J., Velázquez, M., Flores-Ortega, O., Ascacio-Valdés, J. A., Huerta-Ochoa, S., Aguilar, C. N. and Prado-Barragán, L. A. 2017. Solid state fermentation of fig (*Ficus carica* L.) by-products using fungi to obtain phenolic compounds with antioxidant

- activity and qualitative evaluation of phenolics obtained. Process Biochemistry 62: 16-23.
- Celli, G. B., Ghanem, A. and Brooks, M. S.-L. 2016. Optimized encapsulation of anthocyanin-rich extract from haskap berries (*Lonicera caerulea* L.) in calcium-alginate microparticles. Journal of Berry Research 6: 1-11.
- Chan, E.-S., Lee, B.-B., Ravindra, P. and Poncelet, D. 2009. Prediction models for shape and size of ca-alginate macrobeads produced through extrusion—dripping method. Journal of Colloid and Interface Science 338: 63-72.
- Chaudhary, V., Thakur, N., Kajla, P., Thakur, S. and Punia, S. 2021. Application of encapsulation technology in edible films: Carrier of bioactive compounds. Frontiers in Sustainable Food Systems 5: 734921.
- Chean, S. X., Hoh, P. Y., How, Y. H., Nyam, K. L. and Pui, L. P. 2021. Microencapsulation of *Lactiplantibacillus plantarum* with inulin and evaluation of survival in simulated gastrointestinal conditions and roselle juice. Brazilian Journal of Food Technology 24: e2020224.
- Chuang, J. J., Huang, Y. Y., Lo, S. H., Hsu, T. F., Huang, W. Y., Huang, S. L. and Lin, Y. S. 2017. Effects of pH on the shape of alginate particles and its release behavior. International Journal of Polymer Science 2017: 902704.
- Davarcı, F., Turan, D., Ozcelik, B. and Poncelet, D. 2017. The influence of solution viscosities and surface tension on calcium-alginate microbead formation using dripping technique. Food Hydrocolloids 62: 119-127.
- de Moura, S. C. S. R., Berling, C. L., Germer, S. P. M., Alvim, I. D. and Hubinger, M. D. 2018. Encapsulating anthocyanins from *Hibiscus sabdariffa* L. calyces by ionic gelation: Pigment stability during storage of microparticles. Food Chemistry 241: 317-327.
- Demircan, H. and Oral, R. A. 2023. Parameters affecting calcium-alginate bead characteristics: Viscosity of hydrocolloids and water solubility of core material. International Journal of Biological Macromolecules 236: 124011.
- Draget, K. I. and Taylor, C. 2011. Chemical, physical and biological properties of alginates and their biomedical implications. Food Hydrocolloids 25(2): 251-256.

- Essifi, K., Lakrat, M., Berraaouan, D., Fauconnier, M.-L., El Bachiri, A. and Tahani, A. 2021. Optimization of gallic acid encapsulation in calcium alginate microbeads using Box-Behnken experimental design. Polymer Bulletin 78(10): 5789-5814.
- Forysenkova, A. A., Ivanova, V. A., Fadeeva, I. V., Mamin, G. V. and Rau, J. V. 2023. 1H NMR and EPR spectroscopies investigation of alginate cross-linking by divalent ions. Materials 16(7): 2832.
- Gholamian, S., Nourani, M. and Bakhshi, N. 2021. Formation and characterization of calcium alginate hydrogel beads filled with cumin seeds essential oil. Food Chemistry 338: 128143.
- Guo, J. and Kaletunç, G. 2016. Dissolution kinetics of pH responsive alginate-pectin hydrogel particles. Food Research International 88: 129-139.
- Haldar, K. and Chakraborty, S. 2021. Thermohydrodynamic analysis of drop impact calcium alginate gelation process. European Journal of Mechanics B/Fluids 86: 231-242.
- İbanoğlu, E. 2002. Rheological behaviour of whey protein stabilized emulsions in the presence of gum Arabic. Journal of Food Engineering 52(3): 273-277.
- Jeong, C., Kim, S., Lee, C., Cho, S. and Kim, S. B. 2020. Changes in the physical properties of calcium alginate gel beads under a wide range of gelation temperature conditions. Foods 9(2): 180.
- Liu, Y., Zhou, Q., He, Y. M., Ma, X. Y., Liu, L. N. and Ke, Y. J. 2021. Optimization of preparation and properties of *Gardenia* yellow pigment-loaded alginate beads. Korean Journal of Chemical Engineering 38(8): 1669-1675.
- Machado, A. R., Silva, P. M. P., Vicente, A. A., Souza-Soares, L. A., Pinheiro, A. C. and Cerqueira, M. A. 2022. Alginate particles for encapsulation of phenolic extract from *Spirulina* sp. LEB-18: Physicochemical characterization and assessment of in vitro gastrointestinal behavior. Polymers 14(21): 4759.
- Marcillo-Parra, V., Tupuna-Yerovi, D. S., González,
  Z. and Ruales, J. 2021. Encapsulation of bioactive compounds from fruit and vegetable by-products for food application—A review.
  Trends in Food Science and Technology 116: 11-23.

- Mazumder, M. A. J. 2013. Bio-Encapsulation for the immune-protection of therapeutic cells. Advanced Materials Research 810: 1-39.
- Muñiz-Márquez, D. B., Contreras, J. C., Rodríguez, R., Mussatto, S. I., Teixeira, J. A. and Aguilar, C. N. 2016. Enhancement of fructosyltransferase and fructooligosaccharides production by *A. oryzae* DIA-MF in solid-state fermentation using aguamiel as culture medium. Bioresource Technology 213: 276-282.
- Najafi-Soulari, S., Shekarchizadeh, H. and Kadivar, M. 2016. Encapsulation optimization of lemon balm antioxidants in calcium alginate hydrogels. Journal of Biomaterials Science Polymer Edition 27(16): 1631-1644.
- Paoletti, S. and Donati, I. 2022. Comparative insights into the fundamental steps underlying gelation of plant and algal ionic polysaccharides: Pectate and alginate. Gels 8(12): 784.
- Partovinia, A. and Vatankhah, E. 2019. Experimental investigation into size and sphericity of alginate micro-beads produced by electrospraying technique: Operational condition optimization. Carbohydrate Polymers 209: 389-399.
- Ramdhan, T., Ching, S. H., Prakash, S. and Bhandari, B. 2019. Time dependent gelling properties of cuboid alginate gels made by external gelation method: Effects of alginate-CaCl<sub>2</sub> solution ratios and pH. Food Hydrocolloids 90: 232-240.
- Roopa, B. S. and Bhattacharya, S. 2008. Alginate gels
  I. Characterization of textural attributes.
  Journal of Food Engineering 85: 123-131.
- Saifullah, M., Shishir, M. R. I., Ferdowsi, R., Rahman, M. R. T. and Van Vuong, Q. 2019. Micro and nano encapsulation, retention and controlled release of flavor and aroma compounds: A critical review. Trends in Food Science and Technology 86: 230-251.
- Sharifi, E., Rahbar Shahrouzi, J., Jafarizadeh-Malmiri, H., Ghaffari, S. and Baradar Khoshfetrat, A. 2021. Optimization of microencapsulation of metronidazole in alginate microbeads for purpose of controlled release. Polymer Bulletin 79: 8883-8903.
- Song, K., Yan, X., Li, S., Zhang, Y., Wang, H., Wang, L., ... and Liu, T. 2015. Preparation and detection of calcium alginate/bone powder hybrid microbeads for *in vitro* culture of

- ADSCs. Journal of Microencapsulation 32(8): 811-819.
- Ta, N. T. M., Trần, Đ. H. and Huỳnh, K. T. 2022. Encapsulation of Gac oil in alginate bead by dripping method. VNUHCM Journal of Engineering and Technology 5: 1392-1399.
- Tomé, A. C. and da Silva, F. A. 2022. Alginate based encapsulation as a tool for the protection of bioactive compounds from aromatic herbs. Food Hydrocolloids for Health 2: 100051.
- Valente, J. F. A., Dias, J. R., Alves, N. and Sousa, A. 2019. Composite central face design-an approach to achieve efficient alginate microcarriers. Polymers 11(12): 1949.
- Woo, J. W., Roh, H. J., Park, H. D., Ji, C. I., Lee, Y. B. and Kim, S. B. 2007. Sphericity optimization of calcium alginate gel beads and the effects of processing conditions on their physical properties. Food Science and Biotechnology 16(5): 715-721.
- Zakeri, M., Moghadam, H., Samimi, A. and Mohebbi-Kalhori, D. 2019. Optimization of calcium alginate beads production by electrospray using response surface methodology. Materials Research Express 6(9): 095412.
- Zhong, D., Huang, X., Yang, H. and Cheng, R. 2010. New insights into viscosity abnormality of sodium alginate aqueous solution. Carbohydrate Polymers 81(4): 948-952.